

# Effects of focused MeV ion beam irradiation on the roughness of electrochemically micromachined silicon surfaces

Y. S. Ow,<sup>a)</sup> S. Azimi, M. B. H. Breese, E. J. Teo, and D. Mangaiyarkarasi  
*Department of Physics, National University of Singapore, Lower Kent Ridge Road, Singapore 119260, Singapore*

(Received 3 February 2010; accepted 29 March 2010; published 20 April 2010)

The authors compare the effects of focused and broad MeV ion beam irradiation on the surface roughness of silicon wafers after subsequent electrochemical anodization. With a focused beam, the roughness increases rapidly for low fluences and then slowly decreases for higher fluences, in contrast to broad beam irradiation where the roughness slowly increases with fluence. This effect is important as it imposes a limitation on the ability to fabricate smooth surfaces using focused ion beam irradiation. For a given fluence, small variations in the resistivity of an irradiated area may arise due to fluctuations of the focused beam current during irradiation. These small variations in resistivity then give rise to an increased roughness during the electrochemical etching. The roughness may be reduced by increasing the scan speed, which alters the way in which the fluctuations in fluence are averaged out over the irradiated surface. © 2010 American Vacuum Society. [DOI: 10.1116/1.3406130]

## I. INTRODUCTION

Porous silicon created by electrochemical anodization<sup>1</sup> has been traditionally used as a sacrificial material for various modes of micromachining silicon.<sup>2,3</sup> More recently, there is growing interest in semiconductor and insulator patterning and micromachining using high-energy ion beam irradiation.<sup>4-10</sup> Using this approach for silicon micromachining, a focused MeV ion beam, typically protons or helium ions, focused to spot sizes of a few hundreds of nanometers in a nuclear microprobe, is used to irradiate wafers. Irradiation increases *p*-type silicon wafer resistivity by creating point defects along the ion trajectories, which locally reduce the current flow during subsequent electrochemical anodization.<sup>1,11</sup> Different fluence irradiations are produced by repetitively scanning the focused beam a differing number of frames over each area. By varying the fluence, the local resistivity may be controllably varied over a given pattern. Hence during the porous silicon formation via electrochemical anodization, current flow would be reduced by varying amounts at irradiated areas and this result in a varying reduced porous silicon formation rate, thereby creating a surface relief pattern with many different heights on the remaining silicon wafer once the porous silicon has been removed.

Many types of patterned porous silicon and silicon surface structures have been fabricated in this manner, patterned distributed Bragg Reflectors,<sup>5</sup> microturbines,<sup>6</sup> and waveguides.<sup>12</sup> Patterned variable photoluminescence wavelength and intensity<sup>7,8</sup> from porous silicon has also been demonstrated as well. For many applications such as low loss silicon photonic components, highly reflective surfaces, high quality-factor microcavities, one needs to produce as smooth a surface as possible.<sup>12,13</sup> Therefore, it is important to study the underlying causes of surface roughness. Different

applications typically use differing resistivity of *p*-type silicon as the starting material, e.g., silicon-based photonic devices normally use low-doped material (1–10 Ω cm) to minimize optical losses due to free carrier scattering, whereas moderately doped material (0.02 Ω cm) is preferred for machining surface relief patterns with multiheight steps, micromirrors, and holographic surfaces since it is easier to machine a range of differing step heights.

The anodized surface roughness can be reduced by a variety of processes. One such method is to apply an electropolishing pulse after anodization, which has both the benefits of smoothing the surface as well as separating the porous layer from the remaining surface.<sup>11</sup> This may also negate the need to immerse the sample in potassium hydroxide (KOH) to remove the porous silicon. Another procedure is a reduction in surface roughness by thermal oxidation<sup>14,15</sup> and subsequent oxide removal by HF. Small particles of silicon or silicon dioxide remaining on the surface may be removed by megasonic cleaning.<sup>16</sup> However, depending on the application, some of these processes may not be appropriate. For example, the formation of silicon waveguides<sup>12</sup> assumes that the porous silicon remains in place for support so electropolishing is not possible. Thermal oxidation converts the silicon surface to an oxide, thus reducing the remaining silicon thickness, and also will not reduce the surface roughness below several nanometers if the initial roughness is high. It is thus important to minimize the initial roughness of the anodized surface produced by current densities below the electropolishing threshold.

In a different mode of irradiation, a large area, broad beam MeV ion irradiation facility was recently developed for rapid, uniform irradiation of areas up to 3 × 3 cm<sup>2</sup> with high fluence uniformity.<sup>17</sup> There is, however, still an important role for focused beam irradiation, also called proton beam writing where it is easier to encompass a range of different fluences to produce more complex, multilevel structures.

<sup>a)</sup>Electronic mail: g0601170@nus.edu.sg

Moreover, no surface mask is required and better spatial resolution of irradiation may be achieved. Here we compare the roughness produced by focused ion beam irradiation with the roughness produced from a uniform broad area irradiation and characterize the differing behavior in terms of the way, in which the focused beam is scanned over the sample surface.

## II. EXPERIMENT

The process of focused MeV ion beam irradiation of selected areas differs in several respects from other forms of irradiation using focused beams of charged particles. In focused ion beam irradiation systems using keV ions, or electron beam lithography using keV electrons, the beam current is typically very stable, and the focused beam may be rapidly scanned over the sample surface using electrostatic scanning. Any small, slow fluctuations in beam current are uniformly distributed over the sample surface so the area is uniformly irradiated. In comparison, focused MeV ion irradiation has two limiting characteristics.

First, fluctuations of the focused beam current arise from the small variations in accelerator terminal voltage, typically some tens of volts for the highly stabilized singletron accelerator.<sup>18</sup> Even though this is typically a factor of ten times more stable than the more commonly used Van de Graaff accelerator, it still results in a minimum level current fluctuations of 2%–5% with typical frequency components of 50 and 400 Hz.<sup>19</sup>

Second, most nuclear microprobes use magnetic scanning to deflect the focused MeV ion beam over the sample surface since it is difficult to achieve the high field strength needed to scan the beam electrostatically. Magnetic scanning requires the beam to be slowly scanned to avoid hysteresis effects distorting the patterned area. Over the period of a single scanned frame of typically 1 min the beam current fluctuates many times so the fluence is not uniformly distributed. Furthermore, for the commonly used high excitation quadrupole triplet lens configuration<sup>20</sup> with highly asymmetric demagnifications, the horizontal scan direction requires a higher magnetic field owing to the greater lens demagnification in this direction. Even slower scan speeds in the horizontal direction are consequently required to minimize hysteresis effects in the stronger magnetic field compared to the vertical direction. In most microprobes the beam is therefore raster-scanned rapidly in the vertical direction and slowly scanned across the surface in the horizontal direction.

In this work a 2 MeV proton beam of about 1 pA, with a range of 48  $\mu\text{m}$  in silicon, focused to a beam spot of 200 nm was used to irradiate small areas of 0.02  $\Omega\text{ cm}$  *p*-type wafers with different fluences. This wafer resistivity exhibits a slightly reduced porous silicon formation rate at fluences of about  $5 \times 10^{14}/\text{cm}^2$  and this reduces by typically 20% after a fluence of about  $5 \times 10^{15}/\text{cm}^2$  [shown below in Fig. 4(a)], hence this is the fluence range used to observe the effects on surface roughness.

Ga–In eutectic and copper wire were then used to make an electrical contact to the unpolished back wafer surface

and epoxy was used to protect the contact from the HF electrolyte. The front wafer surface was then electrochemically anodized in an electrolyte containing HF(48%):water:ethanol in the ratio of 1:1:2. After the removal of porous silicon, the roughness of the irradiated areas was characterized using an atomic force microscope (AFM) and scanning electron microscope (SEM).

## III. RESULTS

Figures 1(a) and 1(b) show AFM images of two sets of five adjacent 10  $\mu\text{m}$  wide bars irradiated on two different wafers. In Fig. 1(a) the fluence ranges from 1 to  $5 \times 10^{15}/\text{cm}^2$  in increments of  $1 \times 10^{15}/\text{cm}^2$  from right to left, whereas in Fig. 1(b) the fluence ranges from 3 to  $5 \times 10^{15}$  in increments of  $0.5 \times 10^{15}/\text{cm}^2$  from right to left. The two wafers were then etched at a current density of 95  $\text{mA}/\text{cm}^2$  for 90 and 30 s, respectively, to achieve different etch depths. The porous silicon was then removed with KOH, producing a thicker surface relief pattern at more highly irradiated areas because the rate of anodization progressively slows down with increasing fluence. In Fig. 1(b), fluctuations in the beam current during irradiation result in pronounced vertical stripes, clearly observed for the lower fluences at the right side of the image. While well-resolved step heights are observed in Fig. 1(a) between the larger fluence intervals, the smaller steps in Fig. 1(b) are almost lost in the large roughness associated with the vertical stripes.

AFM roughness measurements were carried on each sample. The line profiles across each set of five bars are shown in Figs. 1(c) and 1(d), and roughness values are plotted in Fig. 2(a), labeled as 1a and 1b, respectively. The more deeply etched sample exhibits higher roughness, consistent with Ref. 21 where the roughness of different resistivity wafers versus anodization depth and many other factors was studied. However, for both samples the roughness of the irradiated surfaces initially increases sharply for low fluences, compared to the unirradiated background roughness, then decreases with higher fluences.

In Figs. 3(a) and 3(b) SEM images of a different irradiated pattern are shown. Here the sample was anodized at 12  $\text{mA}/\text{cm}^2$  for 4 min and the porous silicon subsequently removed, producing a checkerboard silicon surface relief pattern. The higher roughness of all the irradiated surfaces compared to the unirradiated region is obvious, in spite of the greater etched depth of the unirradiated regions. An AFM image and line scan across this structure is shown in Figs. 3(c) and 3(d) and roughness measurements recorded from different regions with different fluences are plotted in Fig. 2(a), labeled as 3. Again a rapid increase in roughness for low fluence irradiation is observed, then a decrease at higher fluences.

For comparison, Fig. 2(b) shows roughness measurements for the same wafer resistivity irradiated using a broad beam MeV ion irradiation facility,<sup>17</sup> where the fluence is very uniformly distributed across the wafer surface. Each measurement corresponds to one wafer irradiated with a certain fluence in a small area defined by a surface photoresist pattern,

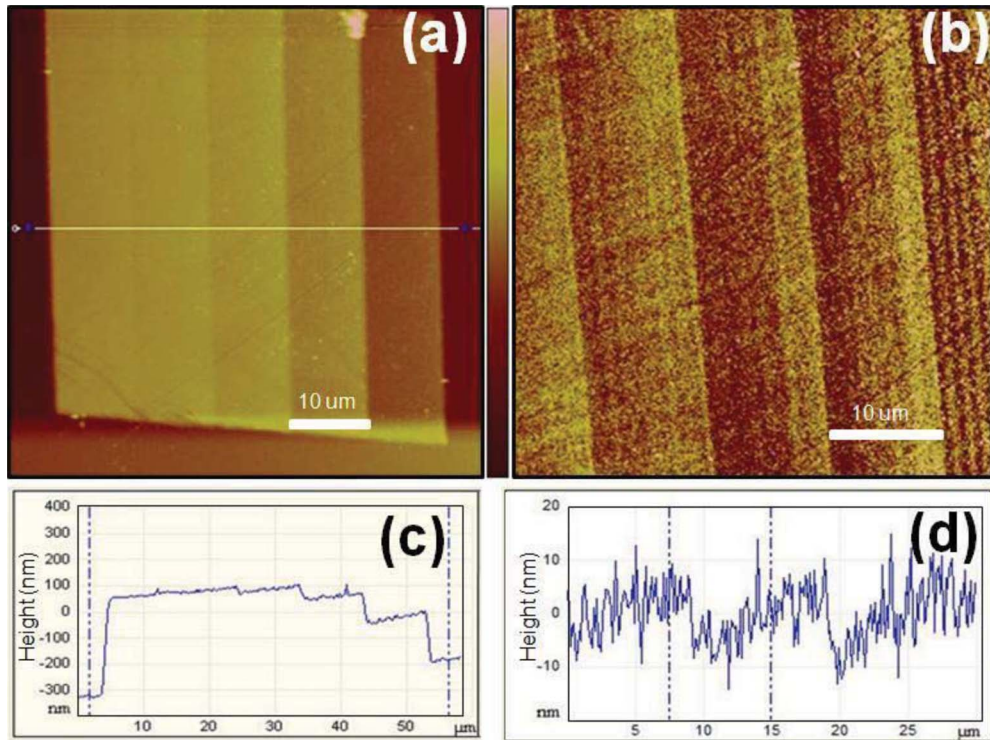


FIG. 1. (Color online) [(a) and (b)] AFM images of two different sets of five adjacent 10  $\mu\text{m}$  wide irradiated bars. The vertical direction of the focused beam during irradiation is shown by the white arrows. [(c) and (d)] AFM line profiles across each pattern in (a) and (b), respectively. The vertical scales are 800 and 40 nm, respectively.

then anodized under similar conditions for 1 or 4 min. Here we are not concerned with comparing the absolute magnitude of roughness, which depends on many other factors related to anodization, only the trend with increasing fluence in different modes of irradiation. In Fig. 2(b) the surface roughness gradually increases with fluence, as expected where the dominant mechanism determining the roughness is the reduced anodization current resulting from increased local resistivity.<sup>21</sup>

#### IV. FACTORS LIMITING ROUGHNESS FOR FOCUSED BEAM IRRADIATION

For all samples irradiated with a focused beam the roughness first increases sharply after a low fluence irradiation and then decreases at higher fluences, in contrast with the behavior observed for broad beam irradiation. This is important as it imposes a limitation on the ability to fabricate smooth surfaces using focused beam irradiation. Here we discuss the

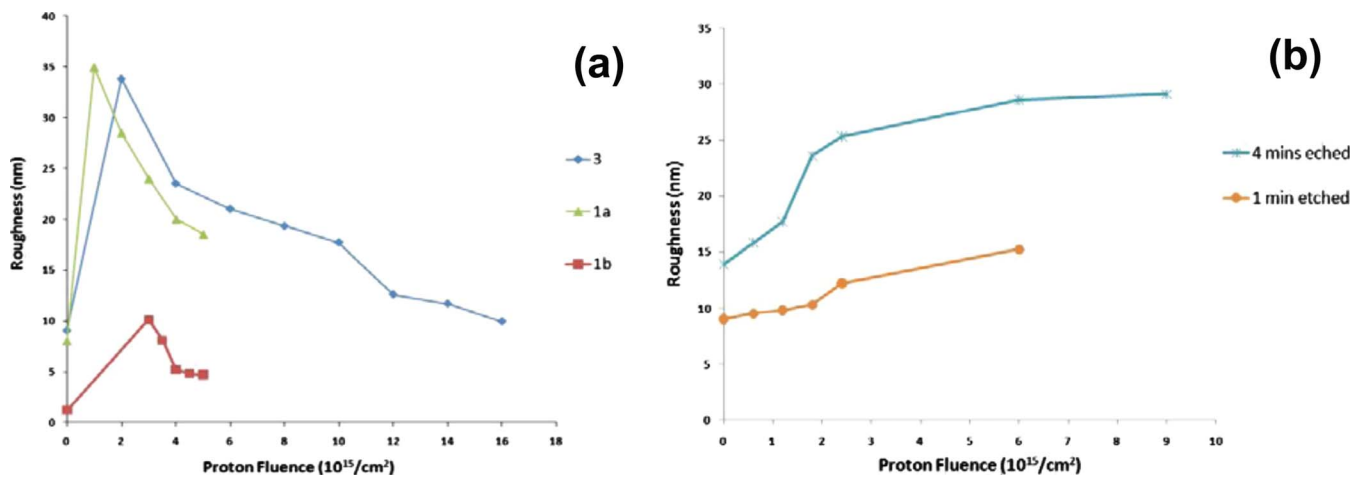


FIG. 2. (Color online) (a) Plot of rms roughness vs fluence for the three samples shown in Figs. 1 and 3, labeled 1a, 1b, and 3, respectively. The AFM rms roughness values are extracted from  $5 \times 5 \mu\text{m}^2$  areas. (b) Plot of the rms roughness vs fluence for two samples irradiated using uniform broad beam ion irradiation. Zero on horizontal axis means the rms roughness measured from the unirradiated background.

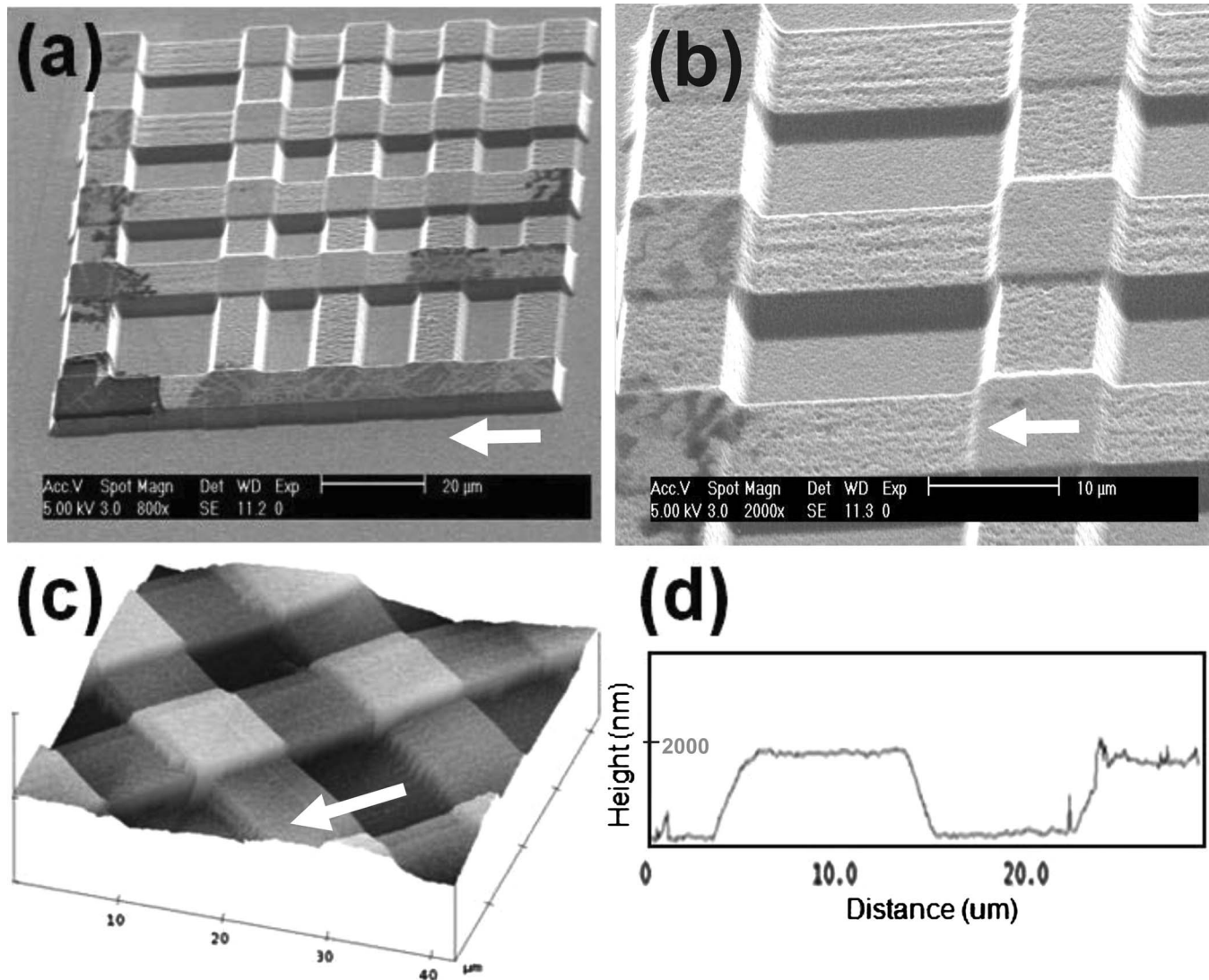


FIG. 3. [(a) and (b)] SEM images of a irradiated pattern with five vertical bars with fluences of 2, 4, 6, 8, and  $10 \times 10^{15}$  protons/cm<sup>2</sup> and overlapped with another five similarly irradiated horizontal bars. The horizontal and vertical bars are each  $10 \times 100 \mu\text{m}^2$  in dimensions. Each bar is spaced at  $10 \mu\text{m}$  from each other except for the two bars with the highest fluence, which were spaced at  $20 \mu\text{m}$  for identification purpose. The vertical direction of the focused beam during irradiation is shown by the white arrows. [(c) and (d)] AFM image and line scan across this structure.

underlying cause of this behavior and how it may be reduced if not completely eliminated. We attribute the roughness behavior of the samples irradiated by focused beam to two factors related to the small fluctuations of the focused beam current during irradiation and the way in which the focused beam is scanned over surface.

One limiting factor is demonstrated in Fig. 4(a), which shows the porous silicon formation rate versus fluence, obtained by taking the ratio between the porous silicon formation rates at an irradiated region compared to that at the unirradiated background. The formation rate changes rapidly at low fluences so the anodization rate at each location, and hence the roughness, is very sensitive to any fluctuations in the low fluence range. The formation rate reduces at higher fluence so the same level of fluctuations in the beam current has a reduced effect on the anodization rate, resulting in a surface with lower roughness. This effect is visible in Fig.

3(b), where stripes along the vertical direction are detected as thickness variations along the edges of the horizontally running bars, caused by the fluctuating beam current during irradiation. These are clearly visible at the low fluence irradiated areas but are not detected when these areas are crossed by orthogonal bars where higher fluence results in smaller fluctuations of the anodization rate.

The second limiting factor leading to the greatly increased surface roughness caused by these vertical stripes observed in Figs. 1 and 3 is the local variations in fluence resulting from the slow scan speed across the horizontal direction. To indicate the importance of making the scan speed as fast as possible relative to the beam current fluctuations, four areas, each of  $50 \times 50 \mu\text{m}^2$ , were irradiated with the same fluence of  $1 \times 10^{15}/\text{cm}^2$  and the same beam current, but with differing scan speeds, hence a different number of frames. No account of hysteresis effects produced by the more rapid

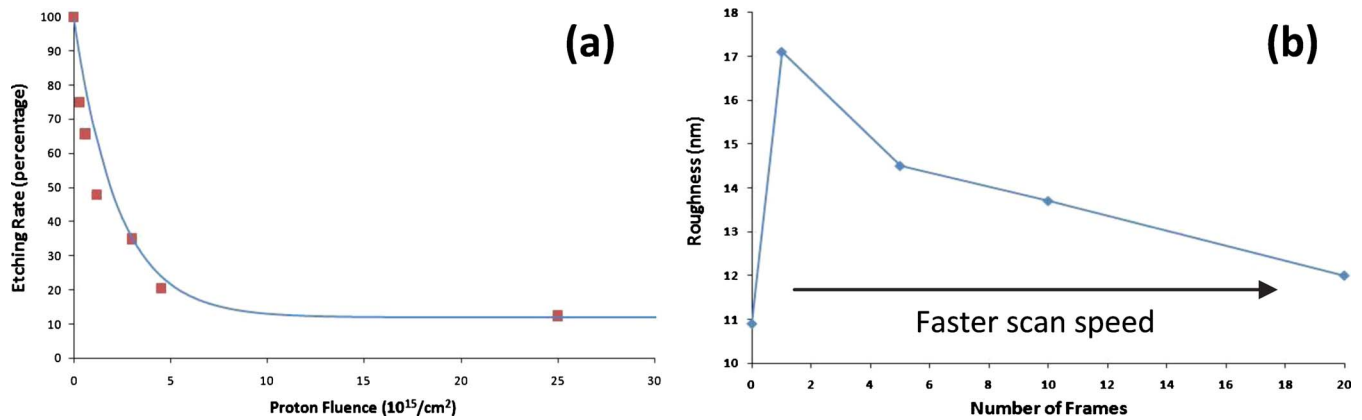


FIG. 4. (Color online) (a) Porous silicon formation rate vs fluence. (b) Measured rms roughness of an irradiated area vs number of frames used to achieve the same fluence in each case. Zero on horizontal axis means the rms roughness measured from the unirradiated background.

beam scanning is taken here. The sample was then anodized at 40 mA for 200 s, the porous silicon was removed and the roughness measured with AFM. The results are plotted in Fig. 4(b). The surface roughness of the irradiated areas clearly reduces for faster scan speeds, i.e., increasing number of frames, owing to better averaging out of the beam current fluctuations.

## V. REMOVAL OF LARGE-SCALE VARIATIONS IN ANODIZATION RATE

A nonuniform etching rate may occur over lateral scales of tens or hundreds of microns due to the influence of the irradiated areas. While this is not a strong influence on the roughness since this effect occurs over larger lateral scales, it is nevertheless a serious problem for our process of machining a range of different surface heights using different fluences. Such nonuniform rate of anodization is present in the structures shown Fig. 1 where the surface of each irradiated bar is sloping. A related problem was described in Ref. 1, arising where a surface mask was used to define certain areas for anodization. A simple explanation for this effect is that the anodization current, which is prevented from reaching the surface at the irradiated regions, is deflected to a region where it can reach the surface. This produces a current gradient across the irradiated regions. Figure 1(d) shows an extreme version of this effect in which the small step heights which should occur between the adjacent different fluences are masked by the slope produced by the deflected hole current. A solution to this problem is shown in the irradiated pattern in Fig. 3 where there are gaps between each irradiated region. The anodization current which is deflected away from the irradiated regions flows to a nearby unirradiated surface, so is not laterally deflected across a large distance nor influence other irradiated areas. This results in flat irradiated surfaces as can be seen in Fig. 3(d), demonstrating that flat surfaces may be achieved by suitably designed patterns.

## VI. CONCLUSIONS

We have studied the effects of focused ion beam irradiation on the surface roughness of electrochemically anodized silicon and compared it to uniform broad beam irradiation. The main factor responsible for large roughness associated with focused beam irradiation is the slow speed of magnetic scanning. With a focused beam the surface roughness is very large at low fluences because this regime is fundamentally more sensitive to any fluctuations in fluence and also because it is difficult to uniformly irradiate a given area with low fluences and a slow scanning speed. At higher fluences the roughness decreases because irradiations become more uniform and also because the sensitivity to nonuniformities is reduced. A faster beam scanning speed averages out any nonuniformities in the irradiated fluence, resulting in lower roughness.

We have also observed the larger scale effects of nonuniform anodization across patterned areas owing to a lateral deflection of the hole current away from the irradiated regions and show how this may be prevented by incorporating gaps in the irradiated pattern through which the displaced hole current may reach the surface.

## ACKNOWLEDGMENT

Funding support by the Singapore Ministry of Education Academic Research Fund Tier 2 under Grant No. T2007B1110 is acknowledged.

- <sup>1</sup>V. Lehmann, *Electrochemistry of Silicon: Instrumentation, Science, Materials and Applications* (Wiley-VCH, Weinheim, Germany, 2002).
- <sup>2</sup>M. Navarro, J. M. Lopez-Villegas, J. Samitier, J. R. Morante, J. Bausells, and A. Merlos, *J. Micromech. Microeng.* **7**, 131 (1997).
- <sup>3</sup>T. E. Bell, P. T. J. Gennissen, D. DeMunter, and M. Kuhl, *J. Micromech. Microeng.* **6**, 361 (1996).
- <sup>4</sup>P. Polesello *et al.*, *Nucl. Instrum. Methods Phys. Res. B* **158**, 173 (1999).
- <sup>5</sup>D. Mangaiyarkarasi, M. B. H. Breese, Y. S. Ow, and C. Vijila, *Appl. Phys. Lett.* **89**, 021910 (2006).
- <sup>6</sup>I. Rajta, S. Z. Szilasi, P. Furjes, Z. Fekete, and C. Ducso, *Nucl. Instrum. Methods Phys. Res. B* **267**, 2292 (2009).
- <sup>7</sup>E. J. Teo, D. Mangaiyarkarasi, M. B. H. Breese, A. A. Bettiol, and D. J. Blackwood, *Appl. Phys. Lett.* **85**, 4370 (2004).

- <sup>8</sup>E. J. Teo, M. B. H. Breese, A. A. Bettiol, D. Mangaiyarkarasi, F. Champeaux, F. Watt, and D. Blackwood, *Adv. Mater. (Weinheim, Ger.)* **18**, 51 (2006).
- <sup>9</sup>F. Menzel, D. Spemann, J. Lenzner, W. Bohlmann, G. Zimmermann, and T. Butz, *Nucl. Instrum. Methods Phys. Res. B* **267**, 2321 (2009).
- <sup>10</sup>F. Nesprias *et al.*, *Nucl. Instrum. Methods Phys. Res. B* **267**, 69 (2009).
- <sup>11</sup>M. B. H. Breese, F. J. T. Champeaux, E. J. Teo, A. A. Bettiol, and D. J. Blackwood, *Phys. Rev. B* **73**, 035428 (2006).
- <sup>12</sup>E. J. Teo, B. Q. Xiong, Y. S. Ow, M. B. H. Breese, and A. A. Bettiol, *Opt. Lett.* **34**, 3142 (2009).
- <sup>13</sup>K. Sugano and O. Tabata, *J. Micromech. Microeng.* **12**, 911 (2002).
- <sup>14</sup>L. Lai and E. A. Irene, *J. Appl. Phys.* **86**, 1729 (1999).
- <sup>15</sup>K. K. Lee, D. R. Lim, L. C. Kimerling, J. Shin, and F. Cerrina, *Opt. Lett.* **26**, 1888 (2001).
- <sup>16</sup>A. A. Busnaina, I. I. Kashkoush, and G. W. Gale, *J. Electrochem. Soc.* **142**, 2812 (1995).
- <sup>17</sup>D. Mangaiyarkarasi, O. Y. Sheng, M. B. H. Breese, V. L. S. Fuh, and E. T. Xioasong, *Opt. Express* **16**, 12757 (2008).
- <sup>18</sup>J. Visser, D. J. W. Mous, A. Gottgang, and R. G. Haitzma, *Nucl. Instrum. Methods Phys. Res. B* **231**, 32 (2005).
- <sup>19</sup>E. J. Teo, M. B. H. Breese, A. A. Bettiol, F. Watt, and L. C. Alves, *J. Vac. Sci. Technol. B* **22**, 560 (2004).
- <sup>20</sup>G. W. Grime, M. Dawson, M. Marsh, I. C. McArthur, and F. Watt, *Nucl. Instrum. Methods Phys. Res. B* **54**, 52 (1991).
- <sup>21</sup>G. Lérondel, R. Romestain, and S. Barret, *J. Appl. Phys.* **81**, 6171 (1997).